


RESEARCH ARTICLE

Temporal Signature of Task-Specificity in Isolated Focal Laryngeal Dystonia

Stefan K. Ehrlich, PhD,¹ Giovanni Battistella, PhD,¹ and Kristina Simonyan, MD, PhD, Dr med^{1,2*} 

¹Department of Otolaryngology—Head & Neck Surgery, Harvard Medical School and Massachusetts Eye and Ear, Boston, Massachusetts, USA

²Department of Neurology—Massachusetts General Hospital, Boston, Massachusetts, USA

ABSTRACT: Background and Objective: Laryngeal dystonia (LD) is focal task-specific dystonia, predominantly affecting speech but not whispering or emotional vocalizations. Prior neuroimaging studies identified brain regions forming a dystonic neural network and contributing to LD pathophysiology. However, the underlying temporal dynamics of these alterations and their contribution to the task-specificity of LD remain largely unknown. The objective of the study was to identify the temporal–spatial signature of altered cortical oscillations associated with LD pathophysiology.

Methods: We used high-density 128-electrode electroencephalography (EEG) recordings during symptomatic speaking and two asymptomatic tasks, whispering and writing, in 24 LD patients and 22 healthy individuals to investigate the spectral dynamics, spatial localization, and interregional effective connectivity of aberrant cortical oscillations within the dystonic neural network, as well as their relationship with LD symptomatology.

Results: Symptomatic speaking in LD patients was characterized by significantly increased gamma synchronization in

the middle/superior frontal gyri, primary somatosensory cortex, and superior parietal lobule, establishing the altered prefrontal-parietal loop. Hyperfunctional connectivity from the left middle frontal gyrus to the right superior parietal lobule was significantly correlated with the age of onset and the duration of LD symptoms. Asymptomatic whisper in LD patients had not no statistically significant changes in any frequency band, whereas asymptomatic writing was characterized by significantly decreased synchronization of beta-band power localized in the right superior frontal gyrus.

Conclusion: Task-specific oscillatory activity of prefrontal-parietal circuitry is likely one of the underlying mechanisms of aberrant heteromodal integration of information processing and transfer within the neural network leading to dystonic motor output. © 2023 International Parkinson and Movement Disorder Society.

Key Words: isolated dystonia; high-resolution EEG; task-specificity

Laryngeal dystonia (LD) is one of the common forms of isolated focal dystonia characterized by involuntary

contractions of the vocal fold muscles, leading to uncontrolled voice breaks and strained, strangled, or breathy quality of voice. A prominent feature of LD is task-specificity as patients experience dystonic symptoms during voiced speech production but not whispering or emotional vocalizations, such as laughing or crying.^{1,2}

The exact pathophysiology of isolated dystonia and particularly the task-specificity of symptoms remain unclear. A recent series of neuroimaging studies have demonstrated distributed brain abnormalities, defining dystonia as a functional and structural neural network disorder.^{3–5} Task-specific dystonias, such as LD, writer's cramp, or musician's dystonia, have been further associated with alterations in brain regions responsible for complex sensorimotor processing, guidance, and integration during movement planning and execution.^{6–11} Among these, the premotor and parietal areas

*Correspondence to: Prof. Kristina Simonyan, Department of Otolaryngology—Head and Neck Surgery, Massachusetts Eye and Ear, Harvard Medical School, 243 Charles Street, Suite 421, Boston, MA 02114, USA; E-mail: kristina_simonyan@meei.harvard.edu

Financial disclosure/conflict of interest: None relevant to this study for all authors. Stefan K. Ehrlich has nothing to disclose. Giovanni Battistella has nothing to disclose. Kristina Simonyan receives funding from the National Institutes of Health (R01NS088160, R01NS124228, R01DC011805, R01DC012545, R01DC019353, P50DC01990, R01DE030464) and the Department of Defense, serves on the Scientific Advisory Board of the Tourette Association of America and the Voice Foundation, and received consulting fees from Jazz Pharmaceuticals Inc. and AbbVie Inc.

Received: 10 April 2023; **Revised:** 6 June 2023; **Accepted:** 28 June 2023

Published online in Wiley Online Library (wileyonlinelibrary.com). DOI: 10.1002/mds.29557

have been identified as critical nodes of the task-specific dystonic network and correlated with the polygenic risk of dystonia development¹² and with the external stressors likely triggering symptom manifestation in susceptible individuals.¹³

The temporal dynamics of these network alterations are, however, less clear. A single electroencephalography (EEG) study in LD patients has reported reduced alpha-band desynchronization in primary somatosensory and premotor cortices during sustained vowel production.¹⁴ Another magnetoencephalography (MEG) study in LD patients has described altered beta and high-gamma activity in the left primary somatosensory cortex, right inferior frontal gyrus, and superior/middle temporal gyri locked to the glottal movement onset during vowel production.¹⁵ While providing initial insights into the temporal features of brain alterations in LD, both studies had several limitations, including small cohorts and simplistic experimental and analytical designs that narrowly focused on the investigation of a few electrodes, brain regions, and frequency bands during the production of a single sustained vowel, a task known to be a less symptom-evoking condition compared to speaking.

More extensive EEG/MEG studies in patients with focal hand dystonia during various manual tasks have determined the presence of abnormal preparatory potential preceding voluntary movement execution and deficiencies in the hand movement-related synchronization and desynchronization in the alpha and beta bands.¹⁶⁻²³ Furthermore, alterations in beta- and gamma-band activity have been identified along with aberrant functional coupling between primary motor and somatosensory cortices and between the parietal cortex and cerebellum.²⁴⁻²⁷ It, however, remains unclear whether the band-specificity and spatial location of altered oscillatory activity are related to dystonic task production and, importantly, how these temporal abnormalities impact the function of the dystonic neural network.³

In this study, we used high-density EEG recordings during a complex, fully symptomatic task production (speaking) and two comparable but asymptomatic tasks (whispering and writing) in LD patients and healthy individuals to determine the spectral dynamics, spatial localization, and effective connectivity between network regions with aberrant cortical oscillations. We hypothesized that selective alteration of temporal information processing in sensorimotor and frontoparietal cortical regions during symptomatic speaking but not asymptomatic tasks is a characteristic feature of the dystonic network dynamics, contributing to the task-specific pathophysiology of LD.

Methods

Study Participants

A total of 51 subjects, including 26 patients with isolated focal LD and 27 healthy controls, participated in

the study. Among these, two LD patients and five healthy controls were excluded from the final analysis because of technical issues during data collection or insufficient quality of EEG recordings. The final cohorts included 24 LD patients (mean age 57.0 ± 12.5 years; 13 females/11 males) and 22 healthy controls (mean age 62.2 ± 8.2 years; 14 females/8 males) (see demographics in Table 1). There were no significant differences in age ($t_{44} = 1.65$, $P = 0.10$) or sex ($\chi^2 = 0.42$, $P = 0.51$) between the groups. All subjects were right-handed and native English speakers. No subject had any past or present history of neurological (except for LD and associated voice tremor), psychiatric, or laryngeal problems as determined by the review of a case history, laryngeal/neurological evaluations, and perceptual

TABLE 1 Demographic characteristics of enrolled participants

Characteristic	LD patients	Healthy controls
Participants (n)	24	22
Age (years; mean \pm SD)	57.0 ± 12.5	62.2 ± 8.2
Sex (female/male)	13/11	14/8
Handedness (Edinburgh Inventory)	Right	
Language	Native English	
Cognitive status (MoCA)	≥ 26	
Centrally acting medications	None	
Last botulinum toxin treatment	>3 months	NA
LD phenotype	17 adductor/6 abductor/1 mixed/11 with voice tremor	NA
LD genotype	22 sporadic/2 familial	NA
LD age of onset (years; mean \pm SD)	45.0 ± 14.4	NA
LD duration (years; mean \pm SD)	12.0 ± 9.0	NA
LD severity		
BFMDRS	5.6 ± 2.2	NA
Voice symptoms (breaks, harshness, breathiness; mean \pm SD)	23.3 ± 12.3	NA

Abbreviations: LD, laryngeal dystonia; SD, standard deviation; MoCA, Montreal Cognitive Assessment; NA, not applicable; BFMDRS, Burke-Fahn-Marsden Dystonia Rating Scale.

analysis of voice and speech recordings.⁴ None of the subjects were carriers of *TOR1A/DYT1*, *THAP1/DYT6*, *TUBB4A/DYT4*, *GNAL/DYT25*, *KMT2B/DYT28*, or *GNAO1* mutations as confirmed by whole-exome sequencing. None of the subjects had any gross radiological abnormalities on their structural magnetic resonance imaging. None of the subjects were on any centrally acting medications prior to or during study participation. Patients who received botulinum toxin injections to manage LD symptoms participated at least 3 months after their last injection when fully symptomatic. All subjects gave written informed consent before study participation, which was approved by the Institutional Review Board of Mass General Brigham.

Data Acquisition

Whole-brain EEG data were acquired using a 128-channel EGI GES 400 system (Magstim, Inc.) at a sampling rate of 1000 Hz. All leads were referenced to channel Cz, and impedances were kept below 50 kΩ following the manufacturer’s recommendations. The higher input impedance of EGI amplifiers compared to amplifiers from other manufacturers allows for higher tolerable scalp impedance while providing an equivalent signal-to-noise ratio.²⁸

During the experiment, all subjects were seated in a comfortable chair in front of a computer monitor and speakers. The experimental stimuli included (1) overt production of English sentences as a symptom-eliciting speech task; (2) whispered production of the same sentences as an asymptomatic but related speech task; and (3) writing of the sentences as an asymptomatic unrelated motor task. The experimental stimuli (eg,

“Sam has a rabbit in his hat”, “Are the olives large?”, “My father has a new car”) were presented to the subject acoustically via speakers one at a time as samples of either voiced or whispered speech production or visually on the computer monitor as samples of writing (Fig. 1A). The sentences comprised a high load of vowels and voiceless consonants to elicit symptoms of adductor and abductor LD, respectively. At each trial, subjects were asked to carefully listen to (3.75 s) or read (5 s) the presented sentence and then cued with an arrow to repeat it as a voiced or whispered sentence (4 s) or write it (5 s) on the paper (Fig. 1A). Each condition was continuously acquired in a block design, with sentences randomized between subjects. Subjects were instructed to remain as still as possible throughout the entire experiment to minimize motion artifacts. A total of 100 speaking, 100 whispering, and 50 writing trials were collected for each subject.

Data Analysis

Data analysis was performed in a hierarchical four-step procedure including: (1) EEG signal preprocessing; (2) spectral topography of cortical oscillations; (3) source localization of statistically significant effects in spectral topography; and (4) effective connectivity of statistically significant source activity (Fig. 1B). EEG data preprocessing and spectral topography analysis were performed using MATLAB (R2021a, MathWorks, Inc.) and the EEGLAB toolbox (version 2021.1).²⁹ Source localization and effective connectivity analyses were performed using SPM12 software. The computation of the lead field matrix (forward model) was performed using OpenMEEG software.³⁰ Statistical analysis of EEG signal

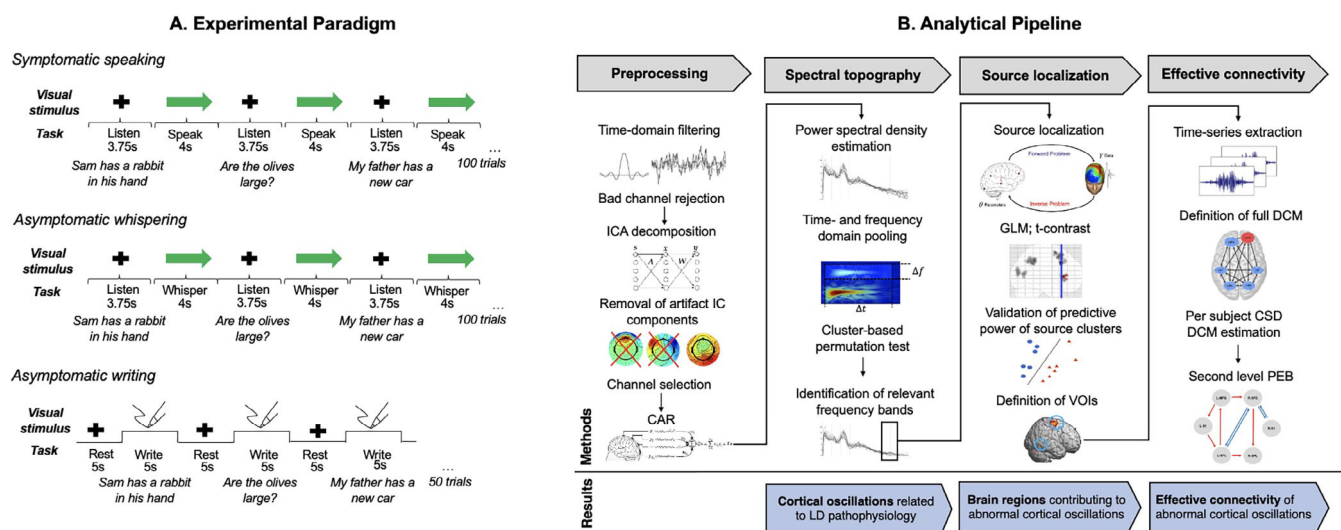


FIG. 1. (A) Schematic illustration of the experimental paradigm for task production, including symptomatic speaking, asymptomatic whispering, and asymptomatic writing. (B) The analytical pipeline of electroencephalography (EEG) data processing, including Preprocessing, Spectral topography, Source localization, and Effective connectivity procedures. ICA, independent component analysis; IC, independent component; CAR, common average referencing; LD, laryngeal dystonia; GLM, general linear model; VOI, volume of interest; DCM, dynamic causal modeling; CSD, cross-spectral density; PEB, parametric empirical Bayes.

differences between the groups was performed using a linear mixed-effect (LME) model in R software (version 4.3.0) with *lme4* and *car* packages.

EEG Signal Preprocessing and Signal Artifact Removal

In each subject, the EEG signal was high-pass filtered using a zero-phase Hamming windowed sinc finite impulse response filter (FIR) with a cutoff frequency of 1 Hz to remove direct current (DC) offsets. To reduce power line noise at 60 Hz in the signals, a zero-phase Hamming windowed sinc notch filter with cutoff frequencies at 55 and 65 Hz was used.

The artifact-contaminated EEG channels were identified using normalized kurtosis, following which spherical interpolation was used to reconstruct rejected channels from the signal of neighboring electrodes. This processing led to a removal of a median of 19 (14.8%) interpolated channels/subject in LD patients and a median of 18 (14.1%) interpolated channels/subject in healthy controls, with no significant differences between groups ($P = 0.54$).

Next, data were downsampled to 250 Hz to reduce the computational load in subsequent processing steps. The remaining artifacts were reduced using independent component analysis (ICA), which was performed using the infomax algorithm (*runica*). The resulting ICs were submitted to the ADJUST plug-in for automatic identification and removal of ICs associated with generic discontinuities, eye movement, facial muscle, and neck tension-related artifacts.³¹ This processing led to the additional removal of a median of 19 (14.8%) ICs/subject in LD patients and 17 (13.3%) ICs/subject in healthy controls, with no significant differences between groups ($P = 0.36$). These removed ICs accounted for 1.6% of the explained variance median in LD patients and 2.9% of the explained variance median in healthy controls, with no significant difference between groups ($P = 0.42$).

Finally, the number of channels was reduced to 70 a priori selected, more centrally located electrodes, which spatially covered broad areas of frontal, central, and parietal brain regions relevant to the dystonia pathophysiology.^{4,32-35} This multi-step artifact removal procedure allowed us to exclude peripheral, motion-prone electrodes without compromising sufficient density of signal sampling from sensorimotor cortical regions of interest (ROIs).

The signal of the final set of 70 electrodes was re-referenced to the common average (CAR) to further reduce signal contamination.³⁶ Segments of EEG recordings between 1 s before the task cue (pre-trial baseline period) and 4 s after the task cue (task period) were extracted as data epochs for further analysis.

Spectral Topography of Cortical Oscillations

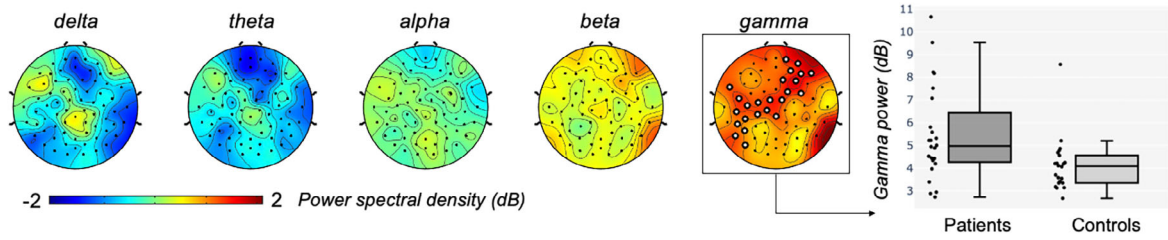
Spectral analysis of each electrode was performed using Welch's power spectral density estimate using 50% overlapping Hamming windows (length 1 s). The size of the fast Fourier transform (FFT) was set to 250 points, resulting in a frequency resolution of 1 Hz. Spectral power was computed for the pre-trial baseline period and the subsequent task period, respectively. Single-trial baseline correction was performed by converting each spectrum to decibels (dB) and subtracting the baseline power from the task power. Next, frequency bins were pooled to yield the average measures of the five standard frequency bands, including delta (1–4 Hz), theta (4–8 Hz), alpha (8–13 Hz), beta (13–30 Hz), and gamma (30–50 Hz).

The Shapiro–Wilk test of normality found that 43% of the data were not normally distributed ($W \geq 0.48$, $P \leq 0.05$). Thus, statistical analysis of between-group and within-group effects was performed using an LME model with groups, experimental tasks, and frequency bands as fixed factors and subjects as random factor. Type II Wald chi-square tests were used to examine the main effects and their interactions at the overall statistical significance of $P \leq 0.01$. Post hoc independent Mann–Whitney tests were performed to determine differences in spectral topography between LD patients and healthy controls at cluster-corrected $P \leq 0.01$ to account for multiple corrections. With a cluster defined as a group of contiguously neighboring significant electrodes, the cluster-based correction was performed with a significance set at $\geq 95\%$ of the largest size of clusters in the randomly permuted data (1000 times) within each band.

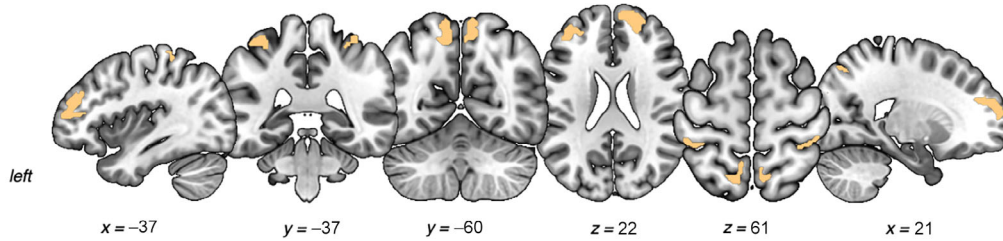
Source Localization

All electrodes were first co-registered using a standard head model and default cortical mesh resolution. The lead field matrix (forward model) was computed using the EEG BEM volume conduction model.³⁷ EEG data were inverted using Greedy Search (GS), an optimized version of the multiple sparse prior (MSP) approach. Source localization analysis focused on the EEG frequency bands found to be significantly different during spectral topography analysis between LD patients and healthy controls. For this, the window of interest was reduced to 0–4000 ms to focus on task-related activity and Hanning windowed to smooth the beginning and end points of the data segments. Subject-specific inverse solutions were computed using a group inversion, including all subjects. Group inversion assumes that the responses in all subjects are explained by the same set of sources, thus circumventing the problem of 'too focal' source activations with consequently little spatial overlap between subjects. The average source activity within the given time window was computed with

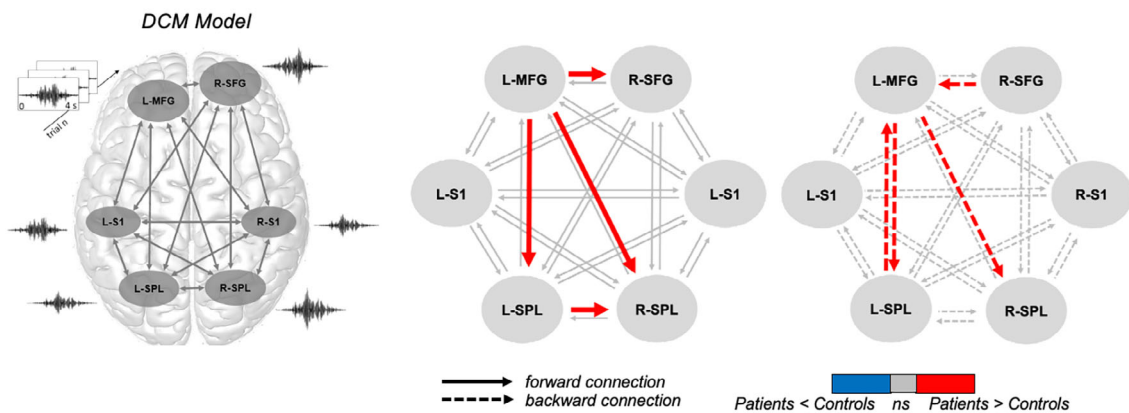
A. Temporal Alterations in Band Power Synchronization during Symptomatic Speaking



B. Spatial Location of Increased Gamma Band Power Synchronization



C. Abnormal Inter-Regional Influences of Gamma Oscillations



D. Clinical Correlations

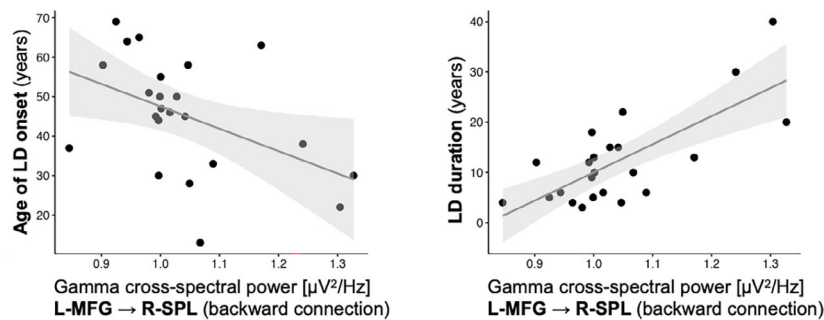


FIG. 2. (A) Temporal alterations in band power synchronization during symptomatic speaking. Group-level differences in spectral power across five frequency bands between patients with laryngeal dystonia (LD) and healthy controls. Significant increases in gamma synchronization are highlighted with a boxplot, with the distribution of the mean gamma band power pooled over the significant channels in both groups. (B) Spatial location of increased gamma band power synchronization. Clusters of significantly different source activity in the gamma frequency band between patients with LD and controls during speaking are shown in a series of brain slices in the MNI (Montreal Neurological Institute) standard space. (C) Abnormal inter-regional influences of gamma oscillations are shown using the second-level parametric empirical Bayes (PEB) analysis for cross-spectral density (CSD) dynamic causal modeling (DCM). The left panel shows the schematic of six regions used in DCM analysis. The middle and right panels show between-group differences in effective connectivity. L-MFG, left middle frontal gyrus; R-SFG, right superior frontal gyrus; R-S1/L-S1, right/left primary somatosensory cortex; R-SPL/L-SPL, right/left superior parietal lobule; ns, non-significant. (D) Significant correlations between clinical features and gamma cross-spectral power connectivity.

default cortical smoothing and used in the general linear model (GLM) to examine the differences between LD patients and healthy controls at $P \leq 0.05$.

Effective Connectivity

To determine the directional influence of one region upon another, the analysis of effective connectivity was performed using statistically significant regions \times frequency bands of between-group source activity and cross-spectral density dynamic causal modeling (DCM). For this, source time series were extracted from ROI, defined as a sphere with a 10-mm radius centered at the highest t voxel value of each cluster. A fully connected model was constructed, with three types of connectivity between all ROIs, including forward or bottom-up connections, backward or top-down connections, and lateral connections targeting all subpopulations.³⁸ The full model parameters were estimated in each subject, and interregional effective connections were defined as probability density functions.

The parametric empirical Bayes (PEB) model³⁹ examined which connections best describe the mean group effect across all subjects and the differences between LD patients and healthy controls. Because the PEB employs the framework of Bayesian statistics, the significance of parameters at the group level is assessed using posterior probabilities (PP) instead of traditional inferential statistics.⁴⁰ P values ≥ 0.80 were considered significant.

Clinical Correlations

Clinical information on the LD symptom onset and duration was obtained during study participation. Symptom severity was assessed using the Burke–Fahn–Marsden Dystonia Rating Scale (BFMDRS). In addition, voice and speech were recorded during the production of sustained vowels, repeated syllables, and a set of 20 symptom-provoking speech sentences in LD patients. Symptom severity was perceptually

quantified by calculating the number of dystonic voice breaks per sentence.⁴¹ LD-associated harshness and breathiness of voice quality were assessed using a visual analog scale (0: no symptoms, 100: most severe symptoms) as described previously.⁴² The mean symptom score used for correlations with EEG-derived features was calculated by averaging all voice symptom measures (ie, breaks, harshness, and breathiness). Correlations between clinical measures and (1) significant topographic clusters of spectral power between-group differences; (2) significant clusters of source power activity; and (3) significant between-group differences in effective connectivity were examined using Spearman's rank correlation coefficients at Bonferroni-corrected $P \leq 0.05$.

Data Sharing

The dataset used and analyzed in the current study is available from the corresponding author upon reasonable request.

Results

The LME analysis found significant group \times task, group \times band, and group \times task \times band interactions (all $P \leq 2 \times 10^{-16}$).

During symptomatic speech production, compared to healthy controls, LD patients had significantly increased synchronization of gamma-band spectral power in the electrodes spanning from the right frontal region to the left parietal region ($U = 139.0$, $P = 0.006$) (Fig. 2A). Spatially, abnormal source activity of the gamma frequency band was localized in the right superior frontal gyrus (SFG), left middle frontal gyrus (MFG), bilateral primary somatosensory cortex (S1), and bilateral superior parietal lobule (SPL) (Fig. 2B,

TABLE 2 Clusters of different source activity between laryngeal dystonia patients and healthy controls

Brain region	t -score	Peak coordinates (x, y, z)	Cluster size (mm ³)
Symptomatic speaking			
R superior frontal gyrus	2.25	14, 62, 16	3352
L middle frontal gyrus	2.12	-36, 46, 20	3368
R primary somatosensory cortex	2.19	40, -36, 60	504
L primary somatosensory cortex	2.18	-40, -38, 60	488
R superior parietal lobule (precuneus)	1.98	10, -70, 54	1736
L superior parietal lobule (precuneus)	1.84	-8, -62, 60	1272
Asymptomatic writing			
R superior frontal gyrus	1.84	14, 62, 18	456

Abbreviations: R, right; L, left.

Table 2). Effective connectivity analysis between these regions showed that LD patients, compared to healthy controls, had significantly increased forward connectivity from the left MFG to the right SFG and bilateral SPL, as well as significantly increased backward connectivity from the left MFG to the right SPL, from the right SFG to the left MFG, and bidirectionally between the left MFG and the left SPL (Fig. 2C). Furthermore, altered backward connectivity from the left MFG to the right SPL was significantly correlated with the age of dystonia onset ($R_S = -0.52, P = 0.009$) and the duration of LD symptoms ($R_S = 0.53, P = 0.007$) (Fig. 2D).

During asymptomatic task production, there were no statistically significant between-group differences in any frequency band during whispering (all $U \geq 205.0, P \geq 0.19$) but significantly decreased synchronization of beta-band power during writing in LD patients compared to healthy controls ($U = 131.0, P = 0.009$)

(Fig. 3A). The corresponding between-group differences in beta-band source activity during writing were localized in the right SFG (Fig. 3B). There were no statistically significant correlations between the temporal characteristics of asymptomatic task production and clinical features of LD.

Discussion

Our findings of abnormal cortical oscillations, their source locations, and corresponding effective connectivity defined spectral-, regional-, and network-level aberrations contributing to LD pathophysiology. Specifically, we determined that increased gamma-band oscillations are a characteristic temporal feature of LD task-specificity, being selectively abnormal during symptomatic speaking but not during speech-related or

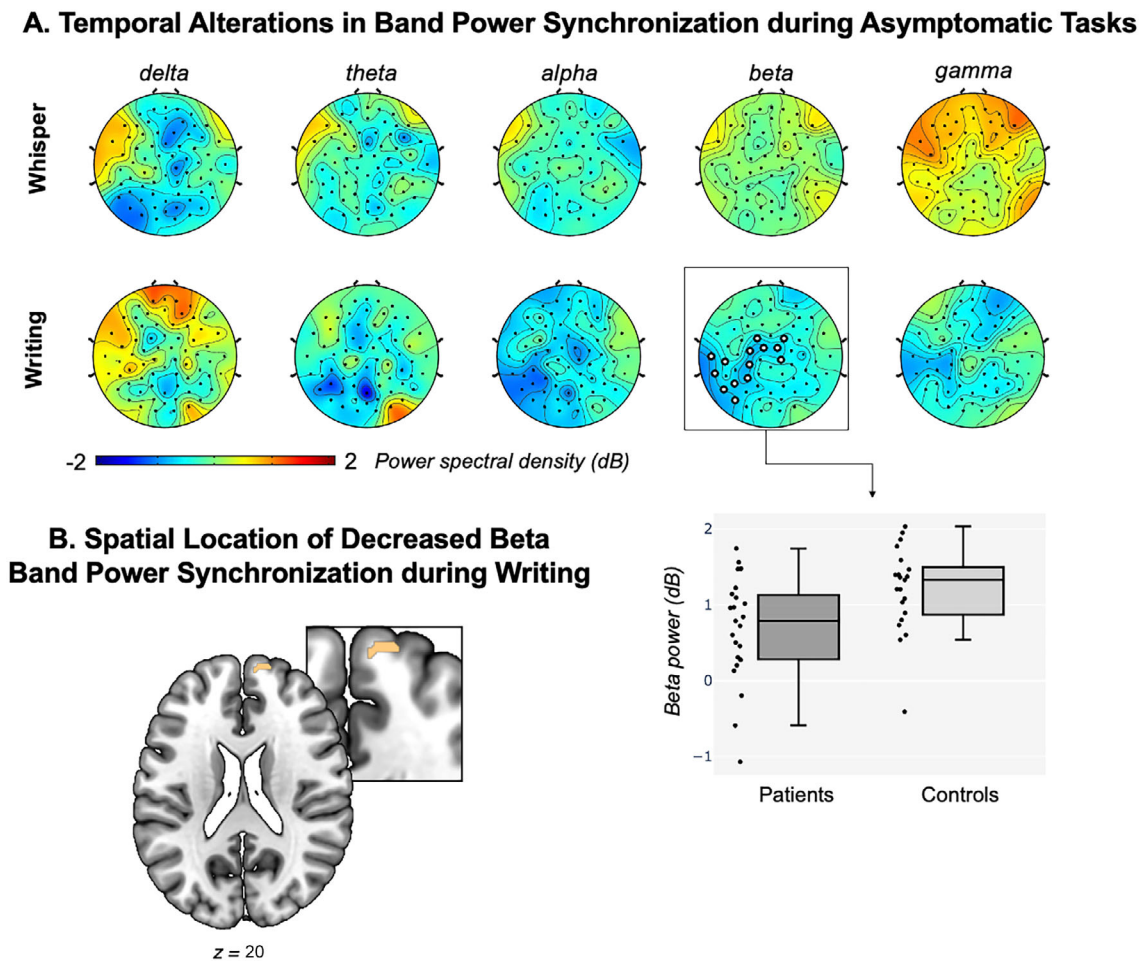


FIG. 3. (A) Temporal alterations in band power synchronization during asymptomatic tasks. Group-level differences in spectral power across five frequency bands between patients with laryngeal dystonia (LD) and healthy controls. Significant decreases in beta synchronization are highlighted with a boxplot, with the distribution of the mean gamma band power pooled over the significant channels in both groups. Results of grand average scalp topography of group differences of spectral power between patients with LD and healthy controls during asymptomatic whisper and writing for five frequency bands. (B) Spatial location of decreased beta band power synchronization. The cluster of significantly different source activity in the beta frequency band between patients with LD and controls during speaking is shown on a brain slice in the Montreal Neurological Institute (MNI) standard space.

unrelated asymptomatic motor behaviors, such as whispering and writing. We further demonstrated that these abnormal oscillations originate from a distributed network of prefrontal, somatosensory, and parietal areas and are characterized by hyperfunctional reciprocal prefrontal-parietal connections and additional inter-hemispheric influences within prefrontal and parietal regions. Together, these findings shed light on the mechanisms of neural dynamics underlying dystonic network activity in LD.

Gamma oscillations are generated by fast-spiking inhibitory interneurons⁴³⁻⁴⁵ and contribute to balancing basal ganglia-thalamo-cortical excitation.^{46,47} These oscillations play an important role in temporal encoding, sensory processes in terms of binding features into a coherent percept, storage and recall of information, and feedback processing, including those during movement execution.⁴⁸⁻⁵³ In line with these physiological characteristics, our data show that disruption of gamma synchronization during LD-symptomatic task production stems not from the classical primary motor cortex but from regions involved in higher-order processes for planning and multimodal integration that are necessary for informing and guiding movement execution.

Specifically, dystonia task-specific abnormalities in gamma-band activity were found to primarily originate from MFG/SFG and SPL, establishing an altered prefrontal-parietal loop. Recent studies in LD and other forms of dystonia have highlighted the involvement of these regions in the disorder pathophysiology by demonstrating structural and functional alterations in the prefrontal areas during sensory discriminatory and cognitive executive processing, as well as their relevance to the disease penetrance.^{9,54-59} Similarly, alterations in the parietal cortex and their associations with the polygenic risk and extrinsic symptom-triggering factors have been implicated in the pathophysiology of task-specific dystonias.^{12,13,60-65} Furthermore, using GABAergic neuro-receptor mapping, loss of inhibition has been demonstrated in these prefrontal and parietal regions across different forms of dystonia.⁶⁶⁻⁶⁹ As gamma oscillations depend on synaptic inhibition driven by GABAergic interneurons,^{44,45} our finding of aberrant gamma synchronization in regions previously reported to have loss of inhibition points to important consequences of altered prefrontal-parietal neural dynamics on the execution of motor programs in patients with dystonia.

The findings of altered effective connectivity offer important insights into the mechanistic processes likely underlying abnormal frontoparietal neural dynamics in LD patients. The DCM model allows for inference on the functional cortical hierarchy between neural populations by modeling three types of extrinsic connections (forward, backward, and lateral) that differ in terms of their origin and neural subpopulation target.⁷⁰ Our finding of increased connectivity in both forward

and backward connections within the frontoparietal information stream points to the altered interplay between different cortical layers and populations of neurons in these regions. Moreover, the directionality of these alterations highlights the prominence of left MFG, which appears to act as a hub influencing the activity of the bilateral SPL and right SFG via both forward and backward connections. Conversely, the left SPL and right SFG directly influence the activity of the left MFG via backward connections, thus closing the loop of abnormal information flow within the dystonic neural network during symptomatic speech production. Notably, the correlations between the MFG-to-SPL hyperfunctional connectivity and LD clinical characteristics suggest greater alterations at a younger age of onset and greater changes with the longer duration of dystonia, further pointing to the significance of prefrontal-parietal connectivity as a potential endophenotypic marker of the disorder.

Other significant increases in gamma-band synchronization during symptomatic speech production in LD patients were found in the bilateral primary somatosensory cortex. As a common pathophysiological feature of dystonia, sensory alterations are thought to contribute to impaired processing of sensory feedback from the dystonic body region and abnormal coupling between sensory input and motor output.^{60,71-73} Our findings suggest that task-specific temporal alterations, specifically within the gamma-band range, likely underlie previously described dystonia-related structural, functional, and neurotransmission abnormalities in the primary somatosensory cortex.

The specificity of these spatial-temporal abnormalities related to the LD symptom-evoking task production is further evident in comparison with a distinct signature of temporal dynamics during the production of asymptomatic behaviors. The latter ranged from no significant alterations during asymptomatic whisper to nominal decreases of beta-band synchronization during asymptomatic writing in LD patients compared to healthy individuals. Beta oscillations play a role in long-range synchronization between neural assemblies,^{74,75} including those relevant to movement execution.⁷⁶⁻⁷⁹ Previous studies in patients with focal hand dystonia have demonstrated altered beta-band event-related synchronization (ERS) across various symptomatic and asymptomatic manual motor tasks.^{17,18,20,80,81} Our finding of similarly deficient beta-band activity during asymptomatic writing in LD patients might reflect a shared pathophysiological feature of globally impaired sensorimotor integration in focal dystonias. Furthermore, localization of beta synchronization changes in the right SFG points to the spatial overlap of multi-band alterations in this region during both symptomatic speaking and asymptomatic writing in LD patients. However, the presence of beta-band deficiency during asymptomatic writing but not

asymptomatic whispering is puzzling. We speculate that the potential differences in motor characteristics of writing versus whispering, as well as the distinct central control of hand movements versus voice production, likely contribute to distinct alterations during these asymptomatic behaviors in LD patients.

While this study defined neural dynamics of brain alterations in LD, its limitations should be acknowledged. It is important to note that gamma-band measurements are known to be sensitive to artifacts due to orofacial and neck muscle activity. We addressed this technical drawback by implementing multi-step processing for the removal of contaminated signal and limiting our analysis to the a priori selected electrodes, which helped exclude motion-prone signal without compromising its sampling from regions of interest. The lack of correlations of altered gamma oscillations with LD symptom severity is an indication that the gamma-band changes are less likely to be driven by speech-related muscle activity. The relevance of identified increases in gamma oscillations to LD pathophysiology rather than muscle artifacts is further supported by findings of prior studies using invasive recordings during deep brain stimulation surgery in patients with other forms of dystonia. For example, narrowband gamma oscillations (60–90 Hz) have been shown to have increased activity in the primary sensorimotor cortex,⁸² globus pallidus,⁸³ and subthalamic nucleus⁸⁴ contributing to abnormal involuntary movements in patients with generalized, cervical, and cranial dystonias. Others found broadband gamma activity of the globus pallidus to correlate with hand movement amplitude and velocity in patients with cervical and segmental dystonia.⁸⁵

In conclusion, our findings of increased gamma oscillations during symptomatic speaking and decreased beta oscillations during asymptomatic writing are characteristic features of temporal alterations of the prefrontal-parietal circuitry in LD pathophysiology. Such task-specific oscillatory activity of prefrontal-parietal circuitry is likely one of the underlying mechanisms of aberrant heteromodal integration of information processing within the neural network leading to dystonic motor output. ■

Acknowledgments: We thank Lena O'Flynn, BA, Alexis Worthley, BA, and Azadeh Hamzehei-Sichani, MA, for help with data acquisition, Vladimir Litvak, PhD, for help with dynamic causal modeling (DCM) analysis, and Sanaz Khosravani, PhD, and Davide Valeriani, PhD, for initial discussions of these data. This study was funded by the grants R01DC019353 and P50DC01990 from the National Institute on Deafness and Other Communication Disorders, National Institutes of Health to K.S.

Data Availability Statement

The dataset used and analyzed in the current study is available from the corresponding author upon reasonable request.

References

- Guiry S, Worthley A, Simonyan K. A separation of innate and learned vocal behaviors defines the symptomatology of spasmodic dysphonia. *Laryngoscope* 2019;129(7):1627–1633.
- Blitzer A, Brin MF, Simonyan K, Ozelius LJ, Frucht SJ. Phenomenology, genetics, and CNS network abnormalities in laryngeal dystonia: a 30-year experience. *Laryngoscope* 2018;128(S(uppl. 1)):S1–S9.
- Lungu C, Ozelius L, Standaert D, et al. Defining research priorities in dystonia. *Neurology* 2020;94(12):526–537.
- Simonyan K, Barkmeier-Kraemer J, Blitzer A, et al. Laryngeal dystonia: multidisciplinary update on terminology, pathophysiology, and research priorities. *Neurology* 2021;96(21):989–1001.
- Simonyan K. Neuroimaging applications in dystonia. *Int Rev Neurobiol* 2018;143:1–30.
- Delnooz CC, Helmich RC, Medendorp WP, Van de Warrenburg BP, Toni I. Writer's cramp: increased dorsal premotor activity during intended writing. *Hum Brain Mapp* 2013;34(3):613–625.
- Gallea C, Horovitz SG, Ali Najee-Ullah M, Hallett M. Impairment of a parieto-premotor network specialized for handwriting in writer's cramp. *Hum Brain Mapp* 2016;37(12):4363–4375.
- Fuertinger S, Simonyan K. Task-specificity in focal dystonia is shaped by aberrant diversity of a functional network kernel. *Mov Disord* 2018;33(12):1918–1927.
- Bianchi S, Fuertinger S, Huddleston H, Frucht SJ, Simonyan K. Functional and structural neural bases of task specificity in isolated focal dystonia. *Mov Disord* 2019;34(4):555–563.
- Hanekamp S, Simonyan K. The large-scale structural connectome of task-specific focal dystonia. *Hum Brain Mapp* 2020 Aug 15;41(12):3253–3265.
- Battistella G, Simonyan K. Top-down alteration of functional connectivity within the sensorimotor network in focal dystonia. *Neurology* 2019;92(16):e1843–e1851.
- Putzel GG, Battistella G, Rumbach AF, Ozelius LJ, Sabuncu MR, Simonyan K. Polygenic risk of spasmodic dysphonia is associated with vulnerable sensorimotor connectivity. *Cereb Cortex* 2018; 28(1):158–166.
- de Lima XL, Simonyan K. The extrinsic risk and its association with neural alterations in spasmodic dysphonia. *Parkinsonism Relat Disord* 2019;65:117–123.
- Khosravani S, Mahnan A, Yeh IL, et al. Atypical somatosensory-motor cortical response during vowel vocalization in spasmodic dysphonia. *Clin Neurophysiol* 2019;130(6):1033–1040.
- Kothare H, Schneider S, Mizuiri D, et al. Temporal specificity of abnormal neural oscillations during phonatory events in laryngeal dystonia. *Brain Commun* 2022;4(2):fca031.
- Yazawa S, Ikeda A, Kaji R, et al. Abnormal cortical processing of voluntary muscle relaxation in patients with focal hand dystonia studied by movement-related potentials. *Brain* 1999;122(Pt 7): 1357–1366.
- Toro C, Deuschl G, Hallett M. Movement-related electroencephalographic desynchronization in patients with hand cramps: evidence for motor cortical involvement in focal dystonia. *Ann Neurol* 2000; 47(4):456–461.
- Tseng YJ, Chen RS, Hsu WY, Hsiao FJ, Lin YY. Reduced motor cortex deactivation in individuals who suffer from writer's cramp. *PLoS One* 2014;9(5):e97561.
- Chen CC, Macerollo A, Heng HM, et al. Low-frequency oscillations in cortical level to help diagnose task-specific dystonia. *Neurobiol Dis* 2021;157:105444.
- Kristeva R, Chakarov V, Losch F, Hummel S, Popa T, Schulte-Mönting J. Electroencephalographic spectral power in writer's cramp patients: evidence for motor cortex malfunctioning during the cramp. *Neuroimage* 2005;27(3):706–714.
- Watanabe T, Yoshioka K, Matsushita K, Ishihara S. Modulation of sensorimotor cortical oscillations in athletes with yips. *Sci Rep* 2021;11(1):10376.

22. Baltazar CA, Machado BS, de Faria DD, et al. Brain connectivity in patients with dystonia during motor tasks. *J Neural Eng* 2020;17(5):056039.
23. Ruiz MH, Strübing F, Jabusch HC, Altenmüller E. EEG oscillatory patterns are associated with error prediction during music performance and are altered in musician's dystonia. *Neuroimage* 2011;55(4):1791–1803.
24. Melgari JM, Zappasodi F, Porcaro C, et al. Movement-induced uncoupling of primary sensory and motor areas in focal task-specific hand dystonia. *Neuroscience* 2013;250:434–445.
25. Hinkley LB, Dolberg R, Honma S, Findlay A, Byl NN, Nagarajan SS. Aberrant oscillatory activity during simple movement in task-specific focal hand dystonia. *Front Neurol* 2012;3:165.
26. Tecchio F, Melgari JM, Zappasodi F, et al. Sensorimotor integration in focal task-specific hand dystonia: a magnetoencephalographic assessment. *Neuroscience* 2008;154(2):563–571.
27. Butz M, Timmermann L, Gross J, et al. Oscillatory coupling in writing and writer's cramp. *J Physiol Paris* 2006;99(1):14–20.
28. Ferree TC, Luu P, Russell GS, Tucker DM. Scalp electrode impedance, infection risk, and EEG data quality. *Clin Neurophysiol* 2001;112(3):536–544.
29. Delorme A, Makeig S. EEGLAB: an open source toolbox for analysis of single-trial EEG dynamics including independent component analysis. *J Neurosci Methods* 2004;134(1):9–21.
30. Gramfort A, Papadopoulos T, Olivi E, Clerc M. OpenMEEG: opensource software for quasistatic bioelectromagnetics. *Biomed Eng Online* 2010;9:45.
31. Mognon A, Jovicich J, Bruzzone L, Buiatti M. ADJUST: an automatic EEG artifact detector based on the joint use of spatial and temporal features. *Psychophysiology* 2011;48:229–240.
32. Valeriani D, Simonyan K. A microstructural neural network biomarker for dystonia diagnosis identified by a DystoniaNet deep learning platform. *Proc Natl Acad Sci U S A* 2020 Oct 20;117(42):26398–26405. <https://doi.org/10.1073/pnas.2009165117>
33. Lokkegaard A, Herz DM, Haagensen BN, Lorentzen AK, Eickhoff SB, Siebner HR. Altered sensorimotor activation patterns in idiopathic dystonia—an activation likelihood estimation meta-analysis of functional brain imaging studies. *Hum Brain Mapp* 2016 Feb;37(2):547–557.
34. Marapin RS, van der Horn HJ, van der Stouwe AMM, Dalenberg JR, de Jong BM, Tijssen MAJ. Altered brain connectivity in hyperkinetic movement disorders: a review of resting-state fMRI. *Neuroimage Clin* 2023;37:103302.
35. Zheng Z, Pan P, Wang W, Shang H. Neural network of primary focal dystonia by an anatomic likelihood estimation meta-analysis of gray matter abnormalities. *J Neurol Sci* 2012;316(1–2):51–55.
36. McFarland DJ, McCane LM, David SV, Wolpaw JR. Spatial filter selection for EEG-based communication. *Electroencephalogr Clin Neurophysiol* 1997;103(3):386–394.
37. Gibson WC. *The Method of Moments in Electromagnetics*. Chapman and Hall/CRC, New York; 2021.
38. Moran RJ, Stephan KE, Seidenbecher T, Pape H-C, Dolan RJ, Friston KJ. Dynamic causal models of steady-state responses. *Neuroimage* 2009;44(3):796–811.
39. Zeidman P, Jafarian A, Seghier ML, et al. A guide to group effective connectivity analysis, part 2: second level analysis with PEB. *Neuroimage* 2019;200:12–25.
40. Kass RE, Raftery AE. Bayes factors. *J Am Stat Assoc* 1995;90(430):773–795.
41. Ludlow CL, Adler CH, Berke GS, et al. Research priorities in spasmodic dysphonia. *Otolaryngol Head Neck Surg* 2008;139(4):495–505.
42. Rumbach AF, Blitzer A, Frucht SJ, Simonyan K. An open-label study of sodium oxybate in spasmodic dysphonia. *Laryngoscope* 2017;127(6):1402–1407.
43. Cardin JA, Carlén M, Meletis K, et al. Driving fast-spiking cells induces gamma rhythm and controls sensory responses. *Nature* 2009;459(7247):663–667.
44. Zich C, Nowak M, Hinson EL, Quinn AJ, Woolrich MW, Stagg CJ. Human motor cortical gamma activity relates to GABAergic signaling and to behaviour. *bioRxiv* 2021. <https://doi.org/10.1101/2021.06.16.448658>
45. Bartos M, Vida I, Jonas P. Synaptic mechanisms of synchronized gamma oscillations in inhibitory interneuron networks. *Nat Rev Neurosci* 2007;8(1):45–56.
46. Berke JD. Functional properties of striatal fast-spiking interneurons. *Front Syst Neurosci* 2011;5:45.
47. Buzsáki G, Wang XJ. Mechanisms of gamma oscillations. *Annu Rev Neurosci* 2012;35:203–225.
48. Crone NE, Miglioretti DL, Gordon B, Lesser RP. Functional mapping of human sensorimotor cortex with electrocorticographic spectral analysis. II. Event-related synchronization in the gamma band. *Brain* 1998;121(Pt 12):2301–2315.
49. Brown P, Marsden C. What do the basal ganglia do? *Lancet* 1998;351(9118):1801–1804.
50. Guan A, Wang S, Huang A, et al. The role of gamma oscillations in central nervous system diseases: mechanism and treatment. *Front Cell Neurosci* 2022;16:962957.
51. Buzsáki G, Chrobak JJ. Temporal structure in spatially organized neuronal ensembles: a role for interneuronal networks. *Curr Opin Neurobiol* 1995;5(4):504–510.
52. Gray CM, Singer W. Stimulus-specific neuronal oscillations in orientation columns of cat visual cortex. *Proc Natl Acad Sci U S A* 1989;86(5):1698–1702.
53. Lisman JE, Idiart MA. Storage of 7 +/- 2 short-term memories in oscillatory subcycles. *Science* 1995;267(5203):1512–1515.
54. Termsarasab P, Ramdhani RA, Battistella G, et al. Neural correlates of abnormal sensory discrimination in laryngeal dystonia. *Neuroimage Clin* 2016;10:18–26.
55. Kimmich O, Molloy A, Whelan R, et al. Temporal discrimination, a cervical dystonia endophenotype: penetrance and functional correlates. *Mov Disord* 2014;29(6):804–811.
56. Maguire F, Reilly RB, Simonyan K. Normal temporal discrimination in musician's dystonia is linked to aberrant sensorimotor processing. *Mov Disord* 2020;35(5):800–807.
57. Khosravani S, Chen G, Ozelius LJ, Simonyan K. Neural endophenotypes and predictors of laryngeal dystonia penetrance and manifestation. *Neurobiol Dis* 2021;148:105223.
58. Zhang M, Huang X, Li B, Shang H, Yang J. Gray matter structural and functional alterations in idiopathic blepharospasm: a multi-modal meta-analysis of VBM and functional neuroimaging studies. *Front Neurol* 2022;13:889714.
59. Huang X, Zhang M, Li B, Shang H, Yang J. Structural and functional brain abnormalities in idiopathic cervical dystonia: a multi-modal meta-analysis. *Parkinsonism Relat Disord* 2022;103:153–165.
60. Simonyan K, Ludlow CL. Abnormal activation of the primary somatosensory cortex in spasmodic dysphonia: an fMRI study. *Cereb Cortex* 2010;20(11):2749–2759.
61. Delnooz CC, Helmich RC, Toni I, van de Warrenburg BP. Reduced parietal connectivity with a premotor writing area in writer's cramp. *Mov Disord* 2012;27(11):1425–1431.
62. Delnooz CC, Pasma JW, Beckmann CF, van de Warrenburg BP. Task-free functional MRI in cervical dystonia reveals multi-network changes that partially normalize with botulinum toxin. *PLoS One* 2013;8(5):e62877.
63. Mohammadi B, Kollwe K, Samii A, Beckmann CF, Dengler R, Münte TF. Changes in resting-state brain networks in writer's cramp. *Hum Brain Mapp* 2012;33(4):840–848.
64. Battistella G, Fuerstinger S, Fleysher L, Ozelius LJ, Simonyan K. Cortical sensorimotor alterations classify clinical phenotype and putative genotype of spasmodic dysphonia. *Eur J Neurol* 2016;23(10):1517–1527.
65. Mantel T, Meindl T, Li Y, et al. Network-specific resting-state connectivity changes in the premotor-parietal axis in writer's cramp. *Neuroimage Clin* 2018;17:137–144.

66. Garibotto V, Romito LM, Elia AE, et al. In vivo evidence for GABA(A) receptor changes in the sensorimotor system in primary dystonia. *Mov Disord* 2011;26(5):852–857.
67. Gallea C, Herath P, Voon V, et al. Loss of inhibition in sensorimotor networks in focal hand dystonia. *Neuroimage Clin* 2018;17:90–97.
68. Simonyan K. Inferior parietal cortex as a hub of loss of inhibition and maladaptive plasticity (Abstract S39). Annual Meeting of the American Academy of Neurology; Boston, MA, USA April 22–28, 2017.
69. Berman BD, Pollard RT, Shelton E, Karki R, Smith-Jones PM, Miao Y. GABAA receptor availability changes underlie symptoms in isolated cervical dystonia. *Front Neurol* 2018;9:188.
70. Felleman DJ, Van Essen DC. Distributed hierarchical processing in the primate cerebral cortex. *Cereb Cortex* 1991;1(1):1–47.
71. Ceballos-Baumann AO, Sheean G, Passingham RE, Marsden CD, Brooks DJ. Botulinum toxin does not reverse the cortical dysfunction associated with writer's cramp. A PET study. *Brain* 1997;120(4):571–582.
72. Lerner A, Shill H, Hanakawa T, Bushara K, Goldfine A, Hallett M. Regional cerebral blood flow correlates of the severity of writer's cramp symptoms. *Neuroimage* 2004;21(3):904–913.
73. Hallett M. Dystonia: a sensory and motor disorder of short latency inhibition. *Ann Neurol* 2009;66(2):125–127.
74. Kopell N, Ermentrout GB, Whittington MA, Traub RD. Gamma rhythms and beta rhythms have different synchronization properties. *Proc Natl Acad Sci U S A* 2000;97(4):1867–1872.
75. Tallon-Baudry C, Mandon S, Freiwald WA, Kreiter AK. Oscillatory synchrony in the monkey temporal lobe correlates with performance in a visual short-term memory task. *Cereb Cortex* 2004;14(7):713–720.
76. Schnitzler A, Gross J. Normal and pathological oscillatory communication in the brain. *Nat Rev Neurosci* 2005;6(4):285–296.
77. Kühn AA, Doyle L, Pogosyan A, et al. Modulation of beta oscillations in the subthalamic area during motor imagery in Parkinson's disease. *Brain* 2006;129(3):695–706.
78. Pfuertscheller G, Neuper C, Brunner C, da Silva FL. Beta rebound after different types of motor imagery in man. *Neurosci Lett* 2005;378(3):156–159.
79. Jenkinson N, Brown P. New insights into the relationship between dopamine, beta oscillations and motor function. *Trends Neurosci* 2011;34(12):611–618.
80. Jin SH, Lin P, Auh S, Hallett M. Abnormal functional connectivity in focal hand dystonia: mutual information analysis in EEG. *Mov Disord* 2011;26(7):1274–1281.
81. Ruiz MH, Senghaas P, Grossbach M, et al. Defective inhibition and inter-regional phase synchronization in pianists with musician's dystonia: an EEG study. *Hum Brain Mapp* 2009;30(8):2689–2700.
82. Miocinovic S, Swann NC, de Hemptinne C, Miller A, Ostrem JL, Starr PA. Cortical gamma oscillations in isolated dystonia. *Parkinsonism Relat Disord* 2018;49:104–105.
83. Sedov A, Popov V, Gamaleya A, et al. Pallidal neuron activity determines responsiveness to deep brain stimulation in cervical dystonia. *Clin Neurophysiol* 2021;132(12):3190–3196.
84. Geng X, Zhang J, Jiang Y, et al. Comparison of oscillatory activity in subthalamic nucleus in Parkinson's disease and dystonia. *Neurobiol Dis* 2017;98:100–107.
85. Brücke C, Huebl J, Schönecker T, et al. Scaling of movement is related to pallidal γ oscillations in patients with dystonia. *J Neurosci* 2012;32(3):1008–1019.

SGML and CITI Use Only
DO NOT PRINT

Author Roles

(1) Research project: A. Conception and Design, B. Organization, C. Execution, D. Data Analysis; (2) Statistical Analysis: A. Design, B. Execution, C. Review and Critique; (3) Manuscript: A. Writing of the First Draft, B. Review and Critique; (4) Other: A. Study Supervision, B. Obtaining Funding.

S.K.E.: 1D, 2A, 2B, 3A.

G.B.: 1D, 2A, 2B, 3B.

K.S.: 1A, 1B, 1C, 2A, 2C, 3B, 4A, 4B.